NOTICE

THIS DOCUMENT HAS BEEN REPRODUCED FROM MICROFICHE. ALTHOUGH IT IS RECOGNIZED THAT CERTAIN PORTIONS ARE ILLEGIBLE, IT IS BEING RELEASED IN THE INTEREST OF MAKING AVAILABLE AS MUCH INFORMATION AS POSSIBLE

NASA

Technical Memorandum **81986**

Simultaneous Measurements of Magnetotail Dynamics by IMP Spacecraft

D. H. Fairfield, R. P. Lepping,
E. W. Hones, Jr., S. J. Bame,
and J. R. Asbridge

AUGUST 1980

SIMULTANEOUS MEASUREMENTS OF MAGNETOTAIL DYNAMICS BY IMP SPACECRAFT

D. H. Fairfield and R. P. Lepping
Planetary Magnetospheres Branch
Laboratory for Extraterrestrial Physics
NASA/Goddard Space Flight Center
Greenbelt, Maryland 20771

E. W. Hones, Jr., S. J. Bame and J. R. Asbridge
University of California
Los Alamos Scientific Laboratory
Los Alamos, NM 87545

ABSTRACT

Eleven traversals of the magnetotail at 30-40 R_E by the IMP-7 and IMP-8 spacecraft occurred while IMP-6 was making magnetotail measurements inside of 33 R_E. Combined magnetic field and plasma data from these spacecraft provide the first demonstration of pressure balance between the high β plasma of the plasma sheet and the strong magnetic fields of the tail lobes. The time variations of this pressure support the view that a southward interplanetary magnetic field enhances the accumulation of energy in a magnetotail energy reservoir. Sometimes the accumulated magnetic energy is rapidly dissipated during a magnetospheric substorm. At other times the dissipation can occur more gradually during ongoing magnetic activity. At such times the energy supplied by the solar wind may even exceed that being dissipated, thus causing the tail energy to increase. In addition to plasma sheet thinnings seen prior to substorm onsets inside $\sim$ 15 R_E, a gradual decrease in plasma β is detected in the deep tail which preceeds onset and the more prominent plasma disappearance that typically accompanies it. The frequency of thinnings and the regions over which they occur indicate that drastic changes in plasma sheet thickness are common features of substorms which occur at all locations across the tail. Several magnetically quiet periods correspond to thick plasma sheets with enhanced B_z components and gradually cooling plasmas.

Introduction

There is widespread agreement that the most dramatic portion of a magnetospheric substorm occurs at the onset of the expansion phase (often referred to as t = 0) when dawn-dusk currents in the magnetotail plasma sheet are diverted through the auroral ionosphere. On the ground this onset is detectable through a sudden brightening of the aurora near midnight and the occurrence of negative magnetic perturbations caused by a westward auroral electrojet. In the near earth magnetotail ($\sim$ 6-15 R_E) this event is characterized by a reconfiguration of the magnetic field and the appearance of newly energized hot plasma. There is, however, no general agreement on why this dramatic event occurs, where the newly detected plasma comes from, and how it is energized.

Events leading up to the onset of the expansion phase of a large substorm are well documented. On the ground, high latitude magnetic field observations indicate that relatively weak currents (with magnetic perturbations below a few hundred γ) flow in the auroral zone and on the polar cap (McPherron, 1970; Iijima and Nagata, 1972; Kisabeth and Rostoker, 1974; Iijima, 1974). These weak precursory currents are associated with a southward component of the interplanetary magnetic field (IMF) (Kisabeth and Rostoker, 1974; Fairfield and Cahill, 1966; Burch, 1973) and they can be described in terms of equivalent current systems such as DP2 (Nishida, 1968; Kisabeth and Rostoker, 1974) or S_q^p (Iijima, 1974). The equivalent currents may correspond to actual Hall currents in the ionosphere (Gizler et al., 1976) which are expected to be driven by plasma convection in the magnetosphere.

Other phenomena occurring prior to t = 0 include the precipitation of energetic particles from the magnetosphere (Pytte et al., 1976a), the equatorward movement of proton aurora in the evening and a simultaneous depression in the field strength at midlatitude ground magnetic observatories which is often interpreted as an increase in the evening ring current (Fukunishi, 1975). This field depression is also detected in the evening by equatorial spacecraft at synchronous orbit and beyond (McPherron, 1972). The depression can be attributed to an increase and/or an inward movement of the dawn-dusk magnetotail currents. An increase in the intensity of this current system increases the tail field strength away from the equatorial plane and builds up magnetic energy in the tail which may subsequently be released during substorms. Energetic particles with gyroradii small relative to the minimum radius of curvature of the field line respond adiabatically to this changing configuration (West et al., 1973); equatorially mirroring particles move earthward in order to remain in the same field strength while those with small pitch angles are constrained to continue moving along more tail-like field lines which cross the equatorial plane at greater distances down the tail (e.g., Sauvaud and Winckler, 1980). Particles with gyroradii large relative to the field line curvature are isotropized and some of them precipitate into the atmosphere (Pytte and West, 1978). Field aligned pitch angle distributions of electrons observed at synchronous orbit prior to t = 0 are reported to be very nearly a necessary and sufficient condition for predicting the onset of a substorm (Baker et al., 1978).

3

As the equatorial field strength decreases prior to onset and the field lines assume their more tail-like configuration, both thermal and superthermal particles of the inner plasma sheet are observed to be confined more closely to the equatorial plane. This process also appears to be caused by a southward IMF (Pytte and West, 1978) and it is often described as plasma sheet thinning (Hones et al., 1971). Although the timing of this thinning relative to t = 0 has been a subject of considerable dispute (e.g., Pytte et al., 1976b and references therein), it appears that thinning is restricted to a region inside $\sim$ 15 R_E prior to t = 0 whereas beyond $\sim$ 15 R_E such thinning is frequently observed at later times (Nishida and Fuji, 1976; Pytte et al., 1976b).

Although the morphology of events prior to onset is relatively clear and has been termed the substorm growth phase, the precursory nature of the phenomena have been disputed. Akasofu et al. (1974) have claimed that detailed auroral observations at latitudes poleward of the usual auroral observatories frequently show onset behavior prior to the t = 0 that would be inferred from auroral zone and lower latitude observations. In these cases growth phase phenomena that would have been considered precursory to a large auroral zone t = 0 can be considered as resulting from earlier, smaller, higher latitude onsets which might be expected to have tail associated effects at greater radial distances.

Akasofu (1980) has recently used the timing of onsets as part of an argument that challenges the concept of energy storage in the magnetotail and its subsequent release as the energy of a magnetospheric substorm. As an alternative he argues that solar wind energy is directly converted into substorm energy without intervening storage in the tail. Proponents of a growth phase have, however, not denied the importance of direct energy input. Hones et al. (1976) reported an instance of fast earthward plasma flow enduring for many hours at the tail's midplane during an interval of continual strong southward IMF. At the earth the magnetic signature of this phenomenon was not substorm-like but consisted, instead, of prolonged moderately intense activity lacking identifiable substorm onset features. Hones et al. proposed that that event exemplified a 'steady-state mode' in which magnetospheric energy dissipation processes respond fairly promptly to changes of the IMF.

4

In a similar manner, Pytte et al. (1978a) have emphasized the distinction between (1) intervals when a southward IMF seems to directly drive continual magnetospheric convection and produce continual magnetic activity ("convection bays") and (2) intervals which are characterized by sudden onsets and the full complement of substorm features. The convection bays are attributed to direct energy input and two cell current systems associated with convection. The substorm onsets are associated with tail current diversion and field aligned current wedges. Results of the present paper will support both these modes of energy input.

In the present work we will adopt the following position with regard to t = 0 and the growth phase. We concur with the view of Pytte et al. (1978b) that magnetotail data in general are less complicated than ground data and that they seem to clearly indicate a dramatic field reconfiguration-plasma energization at a particular time during the course of a substorm. We recognize that more modest onset-like ground effects may occur prior to t = 0, but we suggest that such effects may have different significance when they are not associated with tail effects. Of course it will be impossible to argue that these smaller onset-like events do not have smaller or more spatially limited tail effects not observed by a spacecraft, but that is an inherent limitation associated with point measurements. Overcoming this limitation can be viewed as one of the motivations for the present multi-spacecraft study.

Another goal of the present work is to study changes in the tail energy density during substorms at two locations in the magnetotail. It is well known that the lobes of the magnetotail are characterized by a very tenuous plasma (n $\lesssim 10^{-2}$/cc, Akasofu et al., 1973) and hence plasma β ($\equiv 8\pi nk(T_p+T_e)/B^2$) is very small and the energy density is virtually all in the magnetic field. The plasma sheet, on the other hand, is characterized by a denser, hotter plasma and a lower magnetic field such that typically $\beta > 1$ and the bulk of the energy density is in the thermal plasma. Although plasma and field data have never before been combined to give total energy densities in the magnetotail, it has been presumed that the total pressure would remain constant on going from the lobe to the plasma sheet with the decrease in field pressure being compensated for by an increase in plasma pressure. (In this work we will assume an isotropic plasma pressure (Stiles et al., 1978) and add

5

two thirds of the plasma energy density, corresponding to two transverse degrees of freedom, to the transverse field pressure, $B^2/8\pi$, to obtain the total transverse pressure. We will loosely refer to this quantity as either pressure or energy density.) The present paper confirms the constancy of total pressure although the results require a recalibration of the plasma measurements as discussed below.

Instrumentation and Data Presentation

Data used in this study were taken at times when two IMP spacecraft were simultaneously located within the magnetotail. IMP-6 was launched into an eccentric orbit in 1971 and its apogee point at 33 R_E was in the magnetotail during the October-December periods of 1971-1973. IMP-7 and IMP-8 were placed in more circular geocentric orbits of 30-40 R_E in September 1972 and October 1973 respectively and hence every two weeks these spacecraft made several day traverses through the magnetotail. The data set investigated included 6 of these IMP-7 passes through the magnetotail in October-December 1972 and 5 passes of IMP-8 in November-December 1973. Spatial separations ranged from ∿6 R_E up to several 10's of R_E. The simultaneous data set totaled about 22 days.

Los Alamos plasma measurements on these spacecraft were made by electrostatic analyzers with narrow fan shaped apertures that looked out perpendicular to the spin axis. On all three spacecraft the spin axis was nearly perpendicular to the ecliptic plane. All spacecraft sampled electrons and protons in sixteen logarithmically spaced energy channels. On IMP-6 the energy range of 140 ev-29 kev covered the important part of the positive ion distribution in the magnetotail, but on IMPs 7 and 8 the 80 ev-16 kev range was unable to completely measure the hotter distributions. Electron energy ranges of 13 ev to 18 kev on IMP 6 and 5 ev-14 kev on IMP-7 and IMP-8 covered the bulk of the electron distribution. The analyzer on each spacecraft registered particle counts at 16 energies at each of the various sun-referenced rotation angles during each spacecraft spin. The spin periods and count-sampling sequences for the three satellites were such that 16 x 32 energy-angle arrays of counts for electrons and ions were acquired every ∿ 100 seconds by IMP-6 and 16 x 16 arrays were acquired every ∿ 26 seconds by IMP-7 and IMP-8. See Hones et al. (1976) and Hones (1978) for further descriptions

of these instruments.

Tail magnetic field measurements were made by fluxgate magnetometers which were sampled at the rate of 12.5 measurements/sec (IMP 6) and 25 samples/sec (IMPs 7 and 8). (See Fairfield, 1974, and Mish and Lepping, 1976 for further instrumental details.) Interplanetary magnetic field measurements were obtained by the HEOS-1 and HEOS-2 fluxgate magnetometers at sampling rates of one vector measurement every 48 and 32 seconds respectively (Hedgecock, 1975).

In the initial stage of this study a merged plasma-field data set was created with 15 sec field averages being further averaged over the plasma sampling interval. Plasma parameters such as density, n, and average energy for electrons and ions, E_e and E_p, were plotted along with the AE index, the interplanetary magnetic field solar magnetospheric north-south angle, θ_{IP}, and combined field-plasma quantities such as total pressure and plasma β. These quantities are shown in figure 1a and 15 second magnetotail magnetic field parameters are shown in 1b. The plots illustrate the format to be used extensively in this paper except that subsequent figures will be shown with a somewhat expanded time scale. IMP-6 data will always be drawn with a heavy trace and IMP-7 or 8 data with a lighter trace. The magnetic field is presented in terms of magnitude B, latitude and azimuthal angles θ and ϕ and north-south component B_z. Solar magnetospheric coordinates are used throughout the paper. Spacecraft locations are given at the top of the figure and Z' is the estimated distance from the neutral sheet (Fairfield, 1980).

The solid lines in figure 1 bracket times when IMP-6 was in the tail lobe as indicated by a very low value of β in 1a. Outside these intervals the magnetic field tends to display the greater variability and lower magnitude characteristic of the plasma sheet. When the total pressure is computed from field and plasma the curves become much smoother. (Note that the square root of the total pressure has been plotted to facilitate a direct comparison with the field magnitude.) In the initial stage of this study it was found that total pressure was abnormally high in the plasma sheet. The smooth transition curves such as that in 1a were achieved by decreasing the plasma densities at all 3 spacecraft through multiplication by a factor of 2/3. Everything in

this paper reflects this recalibration of the plasma data.

Magnetotail Pressure Balance

In figure 1 both spacecraft are located in the dusk magnetotail at rather similar distances down the tail. Plasma data are unavailable at IMP-8 prior to 15:00 but after this time the total pressure is very nearly equal at both spacecraft. The poorest agreement occurs when the IMP-8 pressure falls below that of IMP-6 during the geomagnetically disturbed interval 1500-1600. This is undoubtedly due to the inability of IMP-8 to measure the unusually hot ions that are characteristic of such disturbed conditions (Akasofu et al., 1973). During the quieter interval 2100-2200 and in many other cases, the agreement is much better.

Another example confirming pressure balance in the tail is shown in Figure 2a and 2b. At the beginning of the data on November 13-14, 1973 the IMP-6 and 8 spacecraft are at similar downstream distances near the dusk magnetotail boundary, but at different Z' distances and in the opposite hemispheres. Just after 1500 both spacecraft are in the tail lobes following the onset of a substorm (Figure 2b). At 1555 IMP-6 suddenly is engulfed by the expanding plasma sheet and the field strength decreases from $\sim 23 \gamma$ to $< 10 \gamma$. Although noisy telemetry limits the availability of plasma data in the succeeding few hours, the few remaining points in Figure 2a indicate that an increase in plasma pressure compensates for the pressure deficit associated with the low IMP-6 magnetic field. Throughout the remainder of the day the total pressure changes at IMP-6 correspond closely to those at IMP-8 even though IMP-6 remains near the equatorial plane in the high β plasma sheet and IMP-8 remains mostly in the low β tail lobe. At 2000 IMP-6 appears to briefly approach or enter the tail lobe for some unexplained reason, but the increased field pressure is compensated for by a plasma decrease so that the total pressure remains smoothly varying on a scale of 10's of minutes. The maximum pressure difference between the two spacecraft occurs at the end of the interval when the X separation is greatest and IMP-8 is 4.5 R_E further down the tail. Such a radial variation in pressure is well known from lobe magnetic field measurements (e.g., Behannon, 1968) and is very obvious in the simultaneous data studied in this paper. Several examples suggest that

8

equi-pressure surfaces in the tail are not planes perpendicular to the tail axis but rather portions of curved surfaces concave toward the earth.

Although many examples similar to Figures 1 and 2 illustrate the approximate constancy of total pressure in the magnetotail, it is difficult to state quantitatively the degree to which this result holds. Incomplete measurement of the hotter plasma distribution introduces an energy dependent error and means that we cannot always expect to observe an exact pressure balance between different regions. Inexact absolute calibration of the plasma measurements can be another source of error. An instrumental threshold prevents measurement of very small fluxes and may cause an additional error which is especially important during intervals of low pressure. Plasma isotropy may not always hold. In view of these difficulties we estimate from comparisons between two spacecraft and from the smoothness of the transitions from lobe to plasma sheet that pressure balance between the lobes and the plasma sheet has been demonstrated to better than 15%.

Tail Energy Storage, Substorms and the IMF

Whereas previous investigations of tail energy changes associated with substorms have been restricted to periods when the observing spacecraft was in the tail lobe and all of the energy was presumed to be measurable with a magnetometer, we are now able to investigate total energy density changes no matter how the energy is distributed between plasma and field. Furthermore, we can compare the changes at two points in the tail and make more accurate inferences about the total energies involved. Energy change studies are particularly important in view of recent suggestions that tail storage is not an important process in the generation of substorms (Akasofu, 1980).

On December 23, 1973, IMP-6 and IMP-8 were both located in the premidnight quadrant of the southern hemisphere but with IMP-8 about 26 R_E further down the tail. Only magnetic field data are shown in Figure 3 since plasma measurements confirm that all significant energy is in the magnetic field except for the period near 2300 when a dashed line for IMP-6 indicates the total pressure with the plasma contribution included. A large enhancement in the auroral zone currents occurred at 1743 with the onset timing deduced to

9

an accuracy of $\pm$ 2 minutes using midlatitude positive bays at several stations. Simultaneous with this increase is a decrease in the tail field strength at the two spacecraft. At IMP-6 in the near earth tail, the field decreases from 28 γ to 23 γ in the 30 minutes following onset. If we assume that this change is representative of all points across the tail as seems likely due to the frequency and longitudinal distribution of such events, we can calculate the change in energy of the tail near the IMP-6 distance by assuming a cylinder with a typical tail radius 18 R_E and an arbitrary height (X distance) 5 R_E as 1.3 x 10^{21} ergs. At the IMP-8 distance, 35 R_E down the tail, the field change is from 15 γ to 13 γ. Taking a cylinder with R = 20 R_E and X = 5 R_E gives an energy change of 3.6 x 10^{20} ergs for this downstream region. Taking intermediate values for contributions from the tail between 15 and 35 R_E gives a total energy change of at least 4 x 10^{21} ergs. Distributing this over a time of 30 minutes gives a rate of energy loss for the tail of 2 x 10^{18} ergs/sec which is in good agreement with the estimation of energy dissipated by ionospheric currents (AE x 10^{15} = 8x10^{17} ergs/sec, Akasofu, 1980).

Although this event gives strong support to the idea that the tail is an important source of substorm energy, it should be noted that the increase at 1743 on December 23 did not begin from quiet conditions. Appreciable auroral zone currents were flowing prior to this time while the tail field was increasing; energy must have been directly input during this time during a "convection bay" (Pytte et al., 1978a) and as advocated by Akasofu (1980).

The IMF north-south angle, θ_{IP}, measured by HEOS-2 and the interplanetary plasma pressure P_{IP} (King, 1977) are also shown in Figure 3. The angle θ_{IP} shows a slight southward turning before and during the large AE increase. High frequency variations in θ_{IP} are due to the fact that HEOS-2 was in the magnetosheath between 1655 and 1800 at its location X = -9.8, Y = 3.6, Z = 33.3 R_E. Apparently the increase and subsequent collapse of the near earth tail moved the magnetopause and bow shock during this period (Maezawa, 1975).

An example illustrating several common features of IMF-magnetotail behavior is shown in Figure 4. Again both IMP spacecraft are in the tail lobe

with IMP-7 far down the tail near midnight and IMP-6 outbound in the dusk quadrant 23 R_E from the IMP-7 location. After ∿ 0300 the IMF B_z component became increasingly more negative and the tail field was increasing. A pair of substorm onsets were apparent in high and midlatitude ground magnetograms at 0419 ± 2 min and 0439 ± 2 min and a similar pair of decreases in the tail magnetic field strength were seen at IMP-6 with times that were simultaneous within the ground uncertainties. The IMP-7 spacecraft saw corresponding decreases which appear to be delayed by a few minutes. The tail field decreases were from 27 to 20 γ at IMP-6 and 17 γ to 10 γ at IMP-7, numbers which imply a tail energy loss of 6 x 10^{21} ergs, which when distributed over 90 minutes, gives a rate of 10^{18} ergs/sec. Again we note that prior to onset AE values approaching 200 γ occurred in the presence of the southward IMF and increasing tail field; direct input of solar wind energy again must have been occurring. We further note that a sudden northward turning of the IMF was seen by HEOS at a location 3 R_E sunward of the dawn dusk meridian plane 7 minutes prior to the first onset. This means that onset was coincident with the arrival of this discontinuity at the downstream tail boundary, and therefore the data support the idea that northward turnings can trigger substorms (Caan et al., 1977).

Returning to Figure 1a we find several additional examples of tail energy changes during substorms. During the interval shown it is clear that four minima in tail energy occur at 1300, 1720, 2000 and 0040. In all cases except that at 1720, the minima occur following an hour interval when large iono-sphere currents (high AE) have apparently drained the tail of much of its energy. The 1720 minimum occurs at the end of the only interval of northward IMF, a time when solar wind energy input is expected to be a minimum. From the behavior of θ_{IP} it would appear that Akasofu's energy coupling function ε would vary in a manner similar to AE until 1800 hours but it would not duplicate the profiles of the later substorms when θ_{IP} is very steady. The large energy decreases in the tail associated with these latter 2 events along with the sudden tail field decrease and AE increase at 1240 seem to further confirm the importance of tail energy storage in producing substorms. On the other hand the increasing tail field after 1300 in the presence of a southward component of the IMF and significant AE indicates that energy can simultane-ously be directly supplied to the magnetotail and dissipated in the ionosphere.

11

These data are consistent with the idea that energy is constantly being supplied to the magnetotail in the presence of a southward field and energy is dissipated by currents diverted through the auroral ionosphere. Whether the tail energy increases or decreases will depend on the relative magnitude of these competing processes.

It is also interesting to note in Figure 1a that the periods of largest tail field energy occur when both IMF and magnetotail fields have a northward component and either no substorms are occurring (prior to 1100) or substorms are decreasing ($\sim$ 1600). In fact it appears that a substorm is terminated at 1600 by a northward field in the presence of a high tail energy density while substorms at $\sim$ 2000 and 0100 are terminated in the presence of a slightly southward field but when the tail energy density above some "ground state" (Akasofu, 1975) or minimum value has been exhausted. Why this minimum is lower at 0040 than at 2000 is not clear although both spacecraft are slightly further downstream at the later time. All substorms on this day are initiated while the tail field component is southward. This behavior is typical and is consistent with earlier experimental results (Fairfield and Ness, 1970) and with the theoretical idea that the tearing mode is responsible for substorm onset (Schindler, 1974).

We introduce two additional intervals in order to discuss their energy density changes before proceeding with a discussion of additional substorm features. In Figure 5a the IMF suddenly turns southward at 2315. The tail lobe pressure at both spacecraft then increases until a substorm onset at $\sim$ 0001 after which it decreases slightly. The IMF remains slightly southward as the substorm decays and the tail energy density increases slightly. Energy density is higher during the moderate activity between 0200 and 0400 than it was at the time of the initial onset. (The IMP-6 pressure increased gradually as the spacecraft moved inward but the fact that a small time dependent increase occurred can be deduced from IMP-7.) Additional abrupt energy density decreases are seen at IMP-6 after times marked by vertical dashed lines at 0521 and 0901. It is interesting that an IMP-7 lobe decrease seems to begin as early as 0450 and occurs well before the 0510 ground onset. This example along with similar events at 1900 and 2400 in Figure 1, indicates that at least in some cases the deep tail may lose energy before the near

earth onset. This could mean that the deep tail may play a role in substorm onsets even though the onset appears to occur on field lines that cross the equatorial plane inside 15 R_E. Since significant AE values acccompany these decreases, the energy loss may also be another example of the normal balance between energy input and loss. Note that the lobe decrease between 0450 and 0600 at IMP-7 is from 24 γ to 13 γ, a 70% decrease in the lobe energy density which occurred in the presence of an IMF that is mostly northward. A similar large decrease occurs at IMP-7 between 0900 and 1030 and it is associated with a more variable IMF. An abrupt enhancement in the rate of increase in tail pressure seems to correspond to a southward turning of the IMF just after 0700, but the southward interval between 0330 and 0430 did not seem to significantly increase the pressure.

On November 28-29, 1973 (Figure 6) the location of IMP-6 is similar to that on October 14, 1972 (Figure 5) except that it is in the premidnight quadrant and at somewhat higher latitude. Although IMP-6 energy density shows mainly an increase with inward spacecraft motion, tail lobe energy density at IMP-8 supports the idea that tail energy density is determined by that energy supplied by the solar wind when θ_{IP} southward minus that removed by ionospheric dissipation. The IMP-8 field decreases in association with the substorms that begin near 2100 and 0053. The latter onset occurs without a substantially southward IMF and the tail energy density decreases to a value at 0330 that is only half the pre-onset value at 0000. The former onset occurs in the presence of a southward IMF and the field decrease is not as large as that seen later in the presence of the northward field. The lobe field begins increasing at ∼ 2300 as the substorm subsides. The interval of increasing B terminates when the IMF turns suddenly northward near 0000. The abrupt IMP-8 decreases in B at ∼ 0140 and 0250, which interupt the more gradual decrease, are tail boundary crossings. These crossings suggest that the tail radius decreases as the tail field strength decreases, thus confirming that a real decrease in the tail flux occurs as was found by Maezawa (1975).

Substorm Onsets at Different Radial Distances

The characteristic behavior associated with substorm onsets at different

13

radial distances is well illustrated in Figure 5. During the 12 hour interval shown, the inbound IMP-6 spacecraft moves from 20 R_E to 7 R_E geocentric distance in the southern hemisphere of the post midnight quadrant. At the same time the IMP-7 spacecraft is in the northern hemisphere of the premidnight quadrant about 30 R_E down the tail. During this interval IMP-6 detects sudden increases in B_z at 0518 and 0902 (second and third vertical dashed lines) which are typically seen near the time of substorm onsets in the region inside 15 R_E. For the 0518 event the ground magnetograms in the night hemisphere (not shown) indicate an onset time of 0510 ± 2 min in Pi2 pulsation (at Boulder) in midlatitude positive bays (at Fredrickburg) and in negative auroral zone H bays (Churchill and Great Whale). The later event is somewhat more complex in the ground data with an initial midlatitude signature at 0835 followed by a further intensification at mid and auroral latitudes at 0850 ± 5 min. Note that these sudden B_z increases are similar to those seen in the midnight and premidnight sector at synchronous orbit but, as Figure 5 illustrates, at these greater distances such events can occur in the post midnight quadrant.

Ground observations indicate that a third earlier substorm began at 0001 ± 2 min when the IMP-6 spacecraft was at 19 R_E. The B_z component at IMP-6 began a more gradual increase near this time which is characteristic of this greater distance. This type of increase can also be seen at IMP-8 near 0520 and 1000 in association with the later events. These B_z increases all indicate the return to more dipolar field lines as the dawn-dusk tail current is diverted through the ionosphere. This substorm current system can be modeled by a closed loop where a dusk to dawn current in the magnetotail corresponds to a decrease in the preexisting dawn-dusk current. Kamide et al. (1974) find that the field aligned portion of this loop may be more important in producing the B_z increase than the change in the tail portion of the current loop.

The timing of the increase in plasma flux following these three substorms is in agreement with the usual morphology. After the 0001 substorm the plasma reappearance is delayed until 0120 (vertical line in Figure 5a) when the substorm intensity is decaying. Such an 80 minute delay is typical of distances beyond ∿ 15 R_E and such events have been termed "recoveries" by

14

Pytte et al. (1978b). After the 0510 and 0850 substorms the delay is only a few minutes. Such short delay times are characteristic of distances inside $\sim$ 15 R_E and such events have been termed expansions by Pytte et al. Exact time relations between ground and spacecraft onset times are difficult to determine due to uncertainties in determining onset times at both locations. Kamide and McIlwain (1974) find that onset times at ground and synchronous orbit agree within 10 minutes but the space data tends to lag the ground. Pytte et al. (1976b) utilized higher resolution spacecraft measurements and Pi2 pulsations to obtain better ground timing. They found ground effects delayed by about one minute relative to their spacecraft and they used this fact to argue that onsets occur first in the tail. In Figure 5 the arrival of plasma at the spacecraft at 0521 and 0910 is delayed relative to the 0510 and 0850 onsets thus suggesting that even inside 15 R_E, but at higher latitudes, there is a significant delay. This delay is probably an indication that the onset occurs initially in a spatially localized equatorial region with the effects expanding outward. The B_z increases in Figure 5 are uncharacteristically delayed relative to the ground onset. More frequently the B_z increase is simultaneous with ground onset within the few minute timing uncertainties. It would be interesting to observe an onset in the region of its initial development where an induction electric field ($\nabla \times \vec{E} = -\partial\vec{B}/\partial t$) may be important, but it will probably be difficult to identify such an occurrence.

Prior to the 0510 and 0850 onsets, β at IMP-6 exhibits a slow decrease for more than an hour. In fact β achieves a very low value after the 0850 ground onset and before the following recovery. A similar decrease seems to follow the 0835 onset and preceeds the partial recovery a few minutes later. The slow decreases of β are due more to field increases and average energy decreases rather than to any decrease in the number density. In the spectrogram at synchronous orbit shown by Sauvaud and Winkler (1980), the same effect can be seen just prior to 0443 onset in their Figure 6; their > 20 kev ions decrease in intensity while the lower energies increase. Between 0800 and 0850 in Figure 5 the IMP-6 density actually increases as β decreases.

Plasma β increases in each of the three reappearances of the plasma sheet at IMP-6 in Figure 5, but due to the high field strengths during this disturbed time and at these distances close to the earth, β does not attain a

15

value greater than unity. Associated with each plasma reappearance is a
sudden increase in the energetic particle intensity by more than three orders
of magnitude (Anderson and Meng, private communication, 1979). After the
first two increases these particles decay to their previously low level on the
same time scale as the β decrease seen in Figure 5b. It seems likely that
these more energetic particles are responding adiabatically to the changing
field configuration (Sauvaud and Winkler, 1980). In the typical manner
(Akasofu et al., 1973), the average ion energy is higher after the plasma
reappearances ($\sim$ 10 kev) than it was before the decrease (a few kev).

Examples from other figures support the above discussion. Increases in
B_z in the near earth tail lobe are seen in near coincidence with substorm
onset at 1747 in Figure 3, at 0438 and in a data gap between 0423 and 0429 in
Figure 4, and at 2123 and 0053 in Figure 6. Few minute delays at the space-
craft relative to the ground may occur at 1747 in Figure 3, 0423 in Figure 4,
and 2123 in Figure 6. The more gradually increases in B_z in the deep tail can
be seen in each of these 3 figures as well as at the time of the 1200, 1900
and 2400 substorms in Figure 1b. The fields are tail-like with small B_z at
the time of all onsets.

Expansions of the plasma sheet at IMP-6 at 2158 and 0121 in Figure 6 and
0540 in Figure 4 are considerably delayed relative to their substorm onsets.
This is contrary to the prompt expansions more typical of these more earthward
locations and is probably due to the relatively large distances of the
spacecraft from the equatorial plane. Field aligned currents are apparent on
the boundary of the expanding plasma sheet (e.g., Fairfield, 1973) as
perturbations in ϕ at 2158 and 0121 in Figure 6 and at 0120, 0520, and 0905 in
Figure 5a. The increases in ϕ in the southern hemisphere (Figure 5a) indicate
current flowing toward the ionosphere as is usual in the post-midnight
quadrant. A negative $\Delta\phi$ followed by a positive $\Delta\phi$ at 0121 (Figure 6)
indicates a pair of current sheets with the conventional directions for this
pre-midnight region but the positive change at 2158 is unusual for this
location.

Plasma Sheet Thinning

16

One of the most characteristic features of substorms in the magnetotail
is the phenomenon of plasma sheet thinning. The prominence of these events in
the multi-spacecraft data set is a clear confirmation that widespread and
large changes in the dimensions of the plasma sheet are invariably associated
with substorms. Plasma sheet half thicknesses often change from 6-8 R_E to
less than 1 R_E, requiring order of magnitude changes in the total number of
plasma sheet particles. The field-plasma, multi-satellite data set offers an
ideal opportunity for detailed study of such events.

Several examples of plasmas sheet thinnings can be seen in Figure 1 where
pairs of solid vertical lines span intervals when no detectable positive ions
are present at IMP-6. These intervals are clearly associated with substorms,
with the plasma disappearances occurring near the onset time as is typical of
distances beyond ⌁ 15 R_E (Pytte et al., 1976b). A new feature apparent in
Figure 1 is that the beginning of the change toward tail lobe conditions, as
indicated by the decrease in β, begins about an hour before substorm onset and
continues during the interval marked by horizontal dashed lines over the β
trace. This slow decrease may be the deep tail analogue to changing particle
phenomena seen by Baker et al. (1978) at sychronous orbit. The β decrease
also seems to correspond to southward θ_{IP}. In each case there seems to be an
increase in the density jus. before the final disappearance of the plasma. In
the typical manner, the recovery of the plasma sheet is seen at both space-
craft during the recovery of the substorm (Hones et a., 1967) although
considerable geomagnetic activity continues beyond 1500 in the presence of an
expanded plasma sheet. Notice that IMP-8 at a greater distance from the
effective equatorial plane spends less time in the plasma sheet but even this
spacecraft sees an expanded sheet at a distance $Z' = 7.5$ R_E at 2100-2200.

Data from September 30-October 1 shown in Figure 7a and 7b show
additional examples of plasma sheet thinning. At IMP-6 near the equatorial
plane, three intervals of high field centered at 1930, 0030 and 0640
correspond to plasma disappearances or reductions and are associated with the
three intervals of enhanced AE. During the 0640 event the spacecraft is very
close to the midplane as is evidenced by the estimated Z' and the repeated
field reversals that preceed and follow the high field interval. It is rather
unusual that the plasma disappearance at 0625 occurs after the peak in AE

rather than nearer the onset. IMP-7 is close to the dusk boundary early on October 1 and the low fields prior to 0000 are due to intervals within the magnetosheath. It is notable that IMP-7 remains in the plasma sheet at $Z' = 6$ R_E at 0640 while IMP-6 enters the lobe. This occurrence is undoubtedly due largely to the well known fact that the plasma sheet tends to be thicker on the flanks than it is in the center of the tail (Bame et al., 1967). It may also indicate variations of the degree of thinning with distance across the tail. On other occasions such as 1530 in Figure 2 thinnings can be seen near the tail boundaries.

As a final example of plasma sheet thinning we present data on October 28-29, 1972 in Figure 8. Near the beginning of this interval both spacecraft are slightly north of the midplane but heading south. IMP-6 is in the premidnight sector and IMP-7 in the post-midnight sector with a separation vector of ~ 23 R_E. Both spacecraft observe the disappearance of plasma near 0830 as the substorm begins. (Plasma flow at this time has been discussed by Frank and Ackerson [1976].) Both spacecraft see the recovery of the plasma sheet within 6 minutes of each other just after 1100 as the substorm recovers. Although data from the two spacecraft are similar on the large scale there are differences on a smaller scale. Immediately after leaving the tail lobe IMP-7 detects a southward field approaching $\theta = -90^\circ$ for almost one minute, but IMP-6 sees no similar effects. The plasma sheet is probably quite thin prior to this recovery since both spacecraft are in the northern tail lobe but at predicted positions just 0.6 and -0.3 R_E from the neutral sheet. Exactly how thin the plasma sheet becomes can not be said due to inaccuracies in the Z' prediction and the fact that the entire tail may be displaced southward from its average location as is suggested by a northward component of the tail lobe field at both spacecraft. A very thin or else rapidly moving plasma sheet is further suggested by the fact that IMP-8 crosses the current sheet into the southern hemisphere plasma sheet only 15 minutes after it exits the northern tail lobe. Another plasma sheet thinning seems to be associated with the AE increase early on October 29, but since both IMPs are moving away from the equatorial plane it is not possible to unambiguously attribute the lobe entry to thinning.

Another typical feature of plasma sheet thinning illustrated in Figure 8

18

is a relatively gradual disappearance of the plasma prior to 0830 as contrasted to the sudden return after 1100. Other examples of the effect may be seen in Figure 1 (1100 vs 1500; 1900 vs 2000; 2300 vs 0100), Figure 2 (1500 vs 1550) and Figure 7 (1800 vs 2020; 2300 vs 0150). Thus, although exceptions can occur (i.e., the sudden entry at 0620 in Figure 7), it appears that the post substorm plasma sheet is better defined as a high β region with a sharp boundary, whereas at other times there is a broader transition region of $\beta \simeq$ 1 plasma between the lobe and the plasma sheet. Although part of this observational distinction is probably due to more rapid plasma sheet boundary motion past the spacecraft during its recovery, the fact that the field generally reaches a lower value (and β a higher value) after the recovery suggest a actual difference in the post-substorm plasma sheet.

Because of the extreme variations in the plasma sheet volume, it is clear that an efficient source must supply the plasma sheet as it recovers during the substorm recovery. A volume of the tail 40 R_E wide by 10 R_E high and at least 20 R_E down the tail (a volume equal to $2 \times 10^{30} cm^3$) must be filled with a density of at least 0.1 $(cc)^{-1}$ and hence about 2×10^{29} particles must be supplied in a few tens of minutes. For illustrative purposes we note that a process that captured all the particles in a 1 R_E thick boundary layer surrounding the circumference of the tail and having a density $n = 4$ $(cc)^{-1}$ and flowing tailward at 200 km/sec could fill the plasma sheet in about one minute. This is not a realistic expectation since most of these particles continue far downstream.

Configuration of the Quiet Tail

In order to evaluate magnetotail changes associated with substorms it is important to understand the configuration of the quiet tail. This configuration is not easy to determine since it is difficult to distinguish between quiet periods totally unaffected by geomagnetic activity and quiet periods when B_z is large after a substorm or small before a substorm. Extended quiet periods seem to offer the best hope for defining the quiet tail but such intervals are rare and even the most quiet periods will inevitably be influenced by some degree of minor disturbance. It may be hoped that statistical studies which easily incorporate large amounts of data may show

quiet time tendencies, but such studies usually define quiet periods from an instantaneous index such as AE which does not remove the effects due to preceeding or following substorms.

In a statistical study Fairfield and Ness (1970) found a tendency for more flux to cross the equatorial plane during very quiet times (AE < 50). A later study (Fairfield, 1979) showed that a complicating effect was that B_z was larger on the flanks of the tail than near midnight. The quiet time effect was not so prominent in the latter study. Fairfield and Ness (1970) also showed an example of an enhanced northward tail flux during an extended quiet period. They suggested that field lines of the quiet tail were more dipole-like having a larger than normal radius of curvature and occurring in the presence of a less well defined cross tail current sheet.

The most extensive study of the quiet tail was performed by West et al. (1978) who used pitch angle information of energetic electrons to infer the radius of curvature of the midnight field lines. In a study of seven geomagnetically quiet or very quiet days they found two cases where large field lines with large radii of curvature existed out to 15 R_E and five cases where such dipole-like fields existed only out to $\sim$ 10 R_E. The two days with dipole-like field lines at larger distances were indeed the most quiet of the quiet days and hence support the idea that the extremely quiet tail has more flux crossing the equatorial plane. On the other hand, the rarity of these extremely quiet intervals suggest that the more common state of the relatively undisturbed tail is rather distended. After attaining a more dipolar state immediately after a substorm (Fairfield and Ness, 1970) the field lines may return to a more stretched configuration unless extremely quiet conditions prevail. West et al. also noted that their two days with the most dipole-like distant fields were associated with unusually weak tail lobe fields. Since almost all of these seven quiet events were associated with northward IMF, the authors speculate that larger interplanetary pressure caused the more tail-like configurations.

Two additional quiet intervals are included in the figures presented above. On October 1 0800-1600 (Figure 7) and October 28 1200-2200 (Figure 8) two IMP spacecraft measured the quiet magnetotail. In each example both

spacecraft remained in the plasma sheet for most of the interval but in neither case was either spacecraft very near the midnight meridian plane. Both intervals were associated with northward IMF as would be expected during quiet conditions. In both cases each spacecraft detected predominantly northward tail fields with B_z frequently greater than 5γ and θ frequently greater than 45°. Hence both examples support the existence of more dipole-like field lines during quiet times. The qualification must be made that the measurements are not made near the center of the tail where B_z tends to be smaller.

It is also of interest to note the plasma parameters in the quiet tail. In Figure 8, the average ion energy is enhanced in the typical manner (Akasofu et al., 1973) after the 1115 plasma sheet recovery. IMP-6 measured a value of $\sim$ 7 kev and IMP-7 was unable to clearly determine the temperature of this hot plasma. After 1300 very similar values were seen at both spacecraft. Average energies slowly decreased and reached a value of $\sim$ 1.5 kev at about 1800. Average electron energies exhibited similar behavior on a scale almost an order of magnitude less than that of the ions. Densities increased from initial low values of 0.2 up to values of 0.7 at IMP-6. Similarly, on October 1 after the 0130 recovery, IMP-6 detected a low density (0.1) hot (9 kev) plasma which gradually cooled down. IMP-7 at greater distances from the equatorial plane saw plasmas which were denser (n $\sim$ 0.8) and cooler (1-3 kev) for most of this time. At 1300 IMP-6 also suddenly entered this region of cooler (1.5 kev) denser (n $\approx$ 1) plasma. This may be evidence for the more tenuous hotter central plasma sheet and a denser cooler boundary plasma sheet previously seen only at low altitudes (Winningham et al., 1975).

Discussion and Summary

With the above figures we have shown data illustrating much of what is known about the earth's magnetotail. New information has been obtained by computing combined field and plasma parameters for the first time and by observing various phenomena at two locations at the same time. Other information previously deduced with data from a single spacecraft or with only field or plasma data is confirmed with convincing clarity. As in most studies, our examples have been selected for times when quiet or disturbed

21

intervals are relatively well defined. For much of the data not shown the AE index indicates moderate ongoing activity without easily defined substorms. At these t es the tail measurements also typically undergo a variety of changes for which it is difficult to establish unique correspondence with groun events.

Although little has been included in the preceeding sections concerning plasma flows, plasma velocity vectors have been inspected. In general, there is rather little correspondence in the flows observed at the two spacecraft, but this observation can usually be explained by the fact that the spacecraft are in different regions. Hones and Schindler (1979) have recently emphasized the need to be close to the equatorial plane to see characteristic substorm associated flows and we feel that the simultaneous spacecraft data fully support this point of view. It is very unlikely hat two spacecraft would simultaneously be in a very thin downstream plasma sheet where clearly recognizable substorm related flows are found.

In this paper pressure in the magnetotail has been of prime interest. Using combined field and plasma data we have demonstrated the approximate balance of pressure between the high β plasma sheet and the low β tail lobes. Although it is difficult to establish quantitatively the degree to which those pressures balance, we estimate that the result holds to better than 15%. Changes in this pressure during substorms and the characteristics of the plasma and field that produce it constitute the main topic of the paper.

The tail during extremely quiet times is probably characterized by dipole-like field lines which have a relatively large radius of curvature at their equatorial crossing point. The tail energy density is relatively low, the B_z component of the field is large, and the tail current sheet and the plasma sheet are both thick. The plasma sheet is relatively cool and dense with average proton energies beyond 20 R_E of 1-3 kev and densities of 0.2-1.0/cc. Figure 7 and two examples not shown support the low latitude findings of Winningham et al. (1975) that the central region of the plasma sheet tends to be somewhat hotter and more tenuous than a cooler denser boundary plasma sheet. It is difficult to comment on the nature of the boundary between the plasma sheet and the lobe since motions of this boundary

past the slowly moving spacecraft are not common during these very quiet times. Under more typical 'quiet' conditions that actually include a low level of disturbance, the features described above are probably true to a lesser degree as the tail begins to assume features more characteristic of disturbed times.

The features most easily studied during disturbed times are those associated with sudden onset substorms. In this paper we feel we have conclusively confirmed the importance of the magnetotail in supplying the energy for these sudden onset substorms; decreases in tail energy density at two points in the magnetotail at the time of substorm onset are commonly seen and indicate a tail wide energy loss with a magnitude comparable with to an estimate of the energy dissipated during the substorm. On the other hand we note cases of increasing tail energy density during some disturbances which indicate that direct dissipation of solar wind energy is another mode of input. We subscribe to the view of Pytte et al. (1978a) that distinguishes between sudden onset substorms and periods of direct conversion of solar wind energy. Direct input is probably important on longer time scales and during magnetic storms, as proposed by Akasofu (1980), but we see no way that direct conversion can explain the explosive dissipation of energy at substorm onset.

An equivalent way to discuss these modes of energy input is to regard the magnetotail as an energy reservoir whose input is controlled by the IMF and from which energy is lost to the ionosphere and inner magnetosphere by various processes. A southward IMF enhances the rate of input of solar wind energy to the reservoir. Sometimes this energy happens to leave the reservoir at the same rate it is added, or in other words, it is directly transferred to the inner magnetosphere or dissipated in the ionosphere. At other times the energy is added faster than it is removed and the excess energy is stored until a substorm onset. A northward field both decreases the rate of input of solar wind energy and also decreases the rate of dissipation since northward fields seem to terminate geomagnetic activity even if surplus energy remains in the magnetotail. A southward field does not appear to determine the exact time of a substorm onset but rather it leads to the establishment of the more tail-like field configuration with a small B_z field component that seems to be a prerequisite for onset. This observation supports suggestions that the

23

tearing mode instability may be important in substorm onset. We also note that one clear example supports the idea (Caan et al., 1977) that a sudden northward turning of the IMF can provide a substorm triggering effect in a marginally stable magnetotail.

We concur with the view that $\sim$ 15 R_E is a distance that separates an inner region where the plasma sheet thins before substorm onset from an outer region where the plasma sheet thins near the time of onset. Substorm onset and plasma sheet expansion in the inner region are simultaneous (within the few minute ground timing accuracies) if the spacecraft is near the equatorial plane, but this expansion may be delayed as much as a few 10's of minutes if the spacecraft is at high latitudes. The magnetic field B_z component in the inner region increases at the time of onset even if the spacecraft is in the high latitude tail lobes. With few exceptions these events occur simultaneously with ground onset and hence support the view that the associated tail reconfiguration is due to the diversion of tail currents through the ionosphere.

Plasma sheet thinning at greater distances is frequently seen at two spacecraft if they are both in the plasma sheet near the time of onset. Numerous examples confirm earlier evidence (e.g., Hones, 1979) that the plasma sheet thins over a wide range of longitudes and hence undergoes a large change in its volume in association with substorms. Its total thickness probably is less than 1 R_E after onset and it recovers during substorm recovery to a thickness which is frequently at least 14 or 16 R_E. We find that β in the distant plasma sheet often gradually decreases during the hour before onset before the plasma suddenly becomes unmeasurable near the time of onset--a result that is probably related to the change in pitch angle distribution seen at sychronous orbit by Baker et al. (1978) at the same time relative to substorm onset. We note that plasma sheet thinning, at least in the distant tail, may occur while the tail pressure is decreasing (e.g., Figure 1 at 1200, 1900 and 2400, Figure 7 at 2330 and 0620 and Figure 8 at 0800). This fact supports the conclusion of Hones et al. (1971) that the thinning is not caused by a compression or squeezing of the tail. As the plasma sheet disappears at the spacecraft location in the distant tail the density sometimes seems to increase for a very few minutes before it finally disappears. This

observation may be related to passage of a boundary plasma sheet over the spacecraft, although it must either be very thin or else be moving very rapidly if it has an appreciable thickness. The sudden recovery of the distant plasma sheet during substorm recovery is due to passage over the spacecraft of a rapidly advancing boundary moving away from the equatorial plane. This boundary separates a newly heated, unusually hot ($\bar{E}_p \approx 10$ kev), high β plasma sheet from the low β tenuous plasma of the tail lobe.

The implication that plasma sheet thinning is not due to a compression or squeezing of the plasma sheet suggests that alternative causes be investigated. We note that Siscoe (1972) in an investigation of the force balance on a tail in equilibrium argued that an increased tangential drag on the tail should be associated with a thin plasma sheet. This effect might explain the near earth thinning that precedes onset and is associated with a southward field which might be expected to enhance reconnection and increase tangential drag. The deep tail thinning associated with onset may be due to downstream loss of the plasma sheet associated with reconnection at a close in neutral line (Hones, 1977). Siscoe (1972) also noted that a thick plasma sheet is required during a quiet time equilibrium situation. This expectation indeed seems to be in accord with observations.

Another possibility is suggested by the work of Cowley (1978) who investigated the effects of a plasma pressure anisotropy in a two dimensional (no y dependence) current sheet. In the special case of isotropy he found that the plasma sheet thickness varied inversely with the plasma β in the equatorial plane. The current in the plasma sheet was distributed throughout the thickness of the plasma sheet. In the anisotropic cases this current distribution was appreciably affected even for small anisotropies. With $P_{||} > P_{\perp}$ the current was enhanced near the equatorial plane, especially with high β. If β was too high, however, Cowley suggested that a non-adiabatic current layer probably forms near the equatorial plane as the local plasma reaches the limit of the firehose instability. For $P_{\perp} > P_{||}$ the tendency is to broaden the the current layer, but unless β is quite low this $P_{\perp} > P_{||}$ tail is unstable to the mirror instability.

Although existing anisotropy measurements are limited to higher energies,

25

the anisotropies are quite large and it is interesting to speculate on their effects if indeed they persist to low enough energies to influence the plasma pressures. As we have previously noted, electron measurements at sychronous orbit (Baker et al., 1978) and beyond (West et al., 1973; Pytte and West, 1978) have shown that particles are indeed more field aligned in the more tail like fields prior to onset. Energetic protons seem to show the same effect (Sauvaud and Winkler, 1980). The effect seems to be due largely to the adiabatic drift of particles around the earth; the equatorially mirroring particles that drift in a constant field less than $\sim 70\gamma$ are lost from the magnetosphere when they fail to find such low magnetospheric fields near the subsolar point. They are then absent from the tail region outside 8-10 R_E. Although we cannot say whether initially a tail-like field and its associated weak equatorial field strength produces an anisotropic distribution via the drift effect or an initial distribution produces the thin current sheet of the tail-like field, we note that the effects are mutually re-enforcing and may lead to increasingly tail-like fields until an instability occurs. Although field aligned particles dominate the inner magnetosphere prior to onset, the higher latitude trapped particles encounter more sharply bending field lines in the equatorial region. These particles are isotropized when their gyroradii are comparable to the field curvature and hence there is an energy dependent boundary beyond which particles are isotropic. This effect may explain the ~ 15 R_E limit to the presubstorm thinning.

We emphasize that the above discussion is premised on the gradient and curvature drift of the more energetic particles rather than the more numerous lower energy plasma particles. Although such effects are sometimes seen at energies below 10 kev (Sauvard and Winkler, 1980), it is not clear that the large anisotropies at higher energies peresist to low enough energies to produce the moderate pressure anisotropies required.

ACKNOWLEDGMENTS

REFERENCES

Akasofu, S.-I., The roles of the north-south component of the interplanetary magnetic field on large-scale auroral dynamics observed by the DMSP satellite, Planet. Space Sci., 23, 1349, 1975.

Akasofu, S.-I., The solar wind-magnetosphere energy coupling and magnetospheric disturbances, preprint 1980a.

Akasofu, S.-I., E. W. Hones, Jr., S. J. Bame, J. R. Asbridge, and A. T. Y. Lui, Magnetotail and boundary layer plasmas at a geocentric distance of ~ 18 R_E: Vela 5 and 6 observations, J. Geophys. Res., 78, 7257, 1973.

Baker, D. N., P. R. Higbie, E. W. Hones, Jr., and R. D. Belian, High resolution energetic particle measurements at 6.6 R_E: 3. Low energy electron anisotropies and short-term substorm predictions, J. Geophys. Res., 85, 4863, 1978.

Bame, S. J., J. R. Asbridge, H. E. Felthauser, E. W. Hones, and I. B. Strong, Characteristics of the plasma sheet in the earth's magnetotail, J. Geophys. Res., 72, 113, 1967.

Buck, R. M., H. I. West, Jr., and R. G. D'Arcy, Jr., Satellite studies of magnetospheric substorms on August 15, 1968: 7. OGO-5 energetic proton observations-spatial boundaries, J. Geophys. Res., 78, 3103, 1973.

Behannon, K. W., Mapping of the earth's bow shock and magnetic tail by Explorer 33, J. Geophys. Res., 73, 907, 1968.

Burch, J. L., Rate of erosion of dayside magnetic flux based on quantitative study of the dependence of polar cusp latitude on the interplanetary magnetic field, Radio Science, 8, 955, 1973.

Caan, M. N., R. L. McPherron, and C. T. Russell, Characteristics of the association between the interplanetary magentic field and substorms, J. Geophys. Res., 82, 4837, 1977.

Cowley, S. W. H., The effects of pressure anisotropy on the equilibrium structure of magnetic current sheets, Planet. Space Sci., 26, 1037, 1978.

Fairfield, D. H., Magnetic field signatures of substorms on high-latitude field lines in the nighttime magnetosphere, J. Geophys. Res., 78, 1553, 1973.

Fairfield, D. H., Whistler waves observed upstream from collisionless shocks, J. Geophys. Res., 79, 1368, 1974.

Fairfield, D. H., On the average configuration of the geomagnetic tail, J. Geophys. Res., 84, 1959, 1979.

Fairfield, D. H., A statistical determination of the shape and position of the geomagnetic neutral sheet, J. Geophys. Res., 85, 775, 1980.

Fairfield, D. H., and L. J. Cahill, Jr., Transition region magnetic field and polar magnetic disturbances, J. Geophys. Res., 71, 155, 1966.

Fairfield, D. H., and N. F. Ness, Configuration of the geomagnetic tail during substorm, J. Geophys. Res., 75, 7032, 1970.

Fukunishi, H., Dynamic relationship between proton and electron auroral substorms, J. Geophys. Res., 80, 553, 1975.

Frank, L. A., and K. L. Ackerson, Examples of plasma flows within the earth's magnetosphere, in Magnetosphere Particles and Fields, B. M. McCormac ed., D. Reidel Publishing Co., Dordrecht, Holland, 29-36, 1976.

Gizler, V. A., B. M. Kuznetsov, V. A. Sergeev, and D. A. Troshichev, The sources of the polar cap and low latitude bay-like disturbances during substorms, Planet. Space Sci., 24, 1133, 1976.

Hedgecock, P. C., Magnetometer experiments in the European space research organization's HEOS satellites, Space Sci. Instr., 1, 61, 1975.

Hones, E. W., Jr., Substorm processes in the magnetotail: Comments on 'On hot tenuous plasmas, fireballs, and boundary layers in the earth's magnetotail' by L. A. Frank, K. L. Ackerson and R. P. Lepping, J. Geophys. Res., 82, 5633, 1977.

Hones, E. W., Jr., Some characteristics of rapidly flowing magnetotail plasmas: Further comments on 'On hot tenuous plasma, fireball, and boundary layers in the earth's magnetotail' by L. A. Frank, K. L. Ackerson, and R. P. Lepping, J. Geophys. Res., 83 3358, 1978.

Hones, E. W. Jr., Transient phenomena in the magnetotail and their relation to substorms, Space Sci. Rev., 23, 393, 1979.

Hones, E. W., Jr., J. R. Asbridge, S. J. Bame and I. B. Strong, Outward flow of plasma in the magnetotail following geomagnetic bays, J. Geophys. Res., 72, 5879, 1967.

Hones, E. W., Jr., S. Singer, L. J. Lanzerotti, J. D. Pierson, and T. J. Rosenberg, Magnetospheric substorm of August 25-26, 1967, J. Geophys. Res., 76, 2977, 1971.

Hones, E. W., Jr., J. R. Asbridge and S. J. Bame, Time variations of the magnetotail plasma sheet at 18 R_E determined from concurrent measurements by a pair of Vela satellites, J. Geophys. Res., 76, 4402, 1971.

Hones, E. W., Jr., S. B. Bame and J. R. Asbridge, Proton flow measurements in the magnetotail plasma sheet made with IMP-6, J. Geophys. Res., 81, 227, 1976.

Hones, E. W., Jr., and K. Schindler, Magnetotail plasma flows during substorms: A survey with IMP-6 and IMP-8 satellites, J. Geophys. Res., 84, 7155, 1979.

Iijima, T., Development of polar magnetic substorms, Rept. Ionos. Space Res. Japan, 28, 67, 1974.

Iijima, T., and T. Nagata, Signatures for substorm development of the growth
    phase and expansion phase, Planet. Space Sci., 20, 1095, 1972.

Kamide, Y., and C. E. McIlwain, The onset time of magnetospheric substorms
    determined from ground and sychronous satellite records, J. Geophys. Res.,
    79, 4787, 1974.

Kamide, Y., F. Yasuhara, and S.-I., Akasofu, On the cause of northward
    magnetic field along the negative X axis during magnetospheric substorms,
    Planet. Space Sci., 22, 1219, 1974.

King, Joseph H., Interplanetary Medium Book, National Space Science Data
    Center publication, NSSDC/WDC-A-R&S 77-04, Greenbelt, MD, 1977.

Kisabeth, J. L., and G. Rostoker, The expansive phase of magnetospheric
    substorms; 1. Development of the auroral electrojet and auroral arc
    configuration during a substorm, J. Geophys. Res., 79, 972, 1974.

Maezawa, Kiyoshi., Magnetotail boundary motion associated with geomagnetic
    substorms, J. Geophys. Res., 80, 3543, 1975.

McPherron, Robert L., Growth phase of magnetospheric substorms, J. Geophys.
    Res., 75, 5592, 1970.

McPherron, R. L., Substorm related changes in the geomagnetic tail: the growth
    phase, Planet. Space Sci., 20, 1521, 1972.

Mish, W. H., and R. P. Lepping, Magnetic field experiment data processing
    systems: Explorers 47 and 50, GSFC publication X-694-76-158, 1976.

Nishida, A., Geomagnetic Dp2 fluctuations and associated magnetospheric
    phenomena, J. Geophys. Res., 73, 1795, 1968.

Nishida, A., and K. Fujii, Thinning of the near-earth (10-15 R_E) plasma sheet
    preceeding the substorm expansion phase, Planet. Space Sci., 24, 849, 1976.

Pellinen, R. J., and W. J. Heikkila, Observations of auroral fading before breakup, J. Geophys. Res., 83, 4207, 1978.

Pytte, T., H. Trefall, G. Kremser, L. Jalonen, and W. Riedler, On the morphology of energetic ($\geq$ 30 kev) electron precipitation during the growth phase of magnetospheric substorms, J. Atmos. Terr. Phys., 38, 739, 1976a.

Pytte, T., R. L. McPherron, and M. G. Kivelson, H. I. West, Jr., E. W. Hones, Jr., Multiple-satellite studies of magnetospheric substorms: radial dynamics of the plasma sheet, J. Geophys. Res., 81, 5921, 1976b.

Pytte, T., R. L. McPherron, E. W. Hones, Jr., and H. I. West, Jr., Multiple-satellite studies of magnetospheric substorms: Distinction between polar magnetic substorms and convection driven magnetic bays, J. Geophys. Res., 83, 663, 1978a.

Pytte, T., R. L. McPherron, M. G. Kivelson, H. I. West, Jr., and E. W. Hones, Jr., Multiple satellite studies of magnetospheric substorms: Plasma sheet recovery and the poleward leap of auroral zone activity, J. Geophys. Res., 83, 5256, 1978b.

Pytte, T., and H. I. West, Jr., Ground-satellite correlations during presubstorm magnetic field configuration changes and plasma sheet thinning in the near-earth magnetotail, J. Geophys. Res., 83, 3791, 1978.

Sauvaud, J.-A., and J. R. Winckler, Dynamics of plasma, energetic particles, and fields near sychronous orbit in the night time sector during magnetospheric substorms, J. Geophys. Res., 85, 2043, 1980.

Schindler, K., A theory of the substorm mechanism, J. Geophys. Res., 79, 2803, 1974.

Siscoe, G. L., On the plasma sheet contribution to the force balance requirements in the geomagnetic tail, J. Geophys. Res., 77, 6230-6234, 1972.

Stiles, G. S., E. W. Hones, Jr., S. J. Bame, and J. R. Asbridge, Plasma sheet
    pressure anisotropies, J. Geophys. Res., 83, 3166, 1978.

West, H. I., Jr., R. M. Buck, and J. R. Walton, Electron pitch angle
    distributions throughout the magnetosphere as observed on OGO-5, J.
    Geophys. Res., 78, 1064, 1973.

West, H. I., Jr., R. M. Buck, and M. G. Kivelson, On the configuration of the
    magnetotail near midnight during quiet and weakly disturbed periods: state
    of the magnetosphere, J. Geophys. Res., 83, 3805, 1978.

Winningham, J. D., F. Yasuhara, S.-I. Akasofu, and W. J. Heikkila, The
    latitudinal morphology of 10 ev to 10 kev electron fluxes during
    magnetically quiet and disturbed times in the 2100-0300 MLT sector, J.
    Geophys. Res., 80, 3148, 1975.

Figure 1a. Data illustrating how the north-south angle of the interplanetary field, θ_{IP}, is related to the AE index and the magnetized plasmas of the magnetotail as measured on two spacecraft (see text). The square root of the total pressure (field plus plasma) is shown along with plasma β, ion density n and average energy energy of ions (E_p) and electrons E_e.

Figure 1b. Magnetic field magnitude B and field component B_z along with latitude and azimuthal magnetic field angles θ and ϕ for the time interval of Figure 1a. Vertical lines span the time intervals when IMP-6 was resident in the low β tail lobe when the plasma sheet became thin during three substorms. Horizontal dashed lines indicate periods of decreasing β prior to each substorm onset.

Figure 2a. Combined field and plasma data in the format of Figure 1a. The close correspondence of pressures in the high β plasma sheet measured by IMP-6 and the low β tail lobe measured by IMP-8 demonstrate the pressure balance between these two regions.

Figure 2b. Magnetic field parameters observed on two spacecraft in the format of Figure 1b. A thin plasma sheet during the expansion phase of a substorm near the dusk magnetotail boundary is indicated by the observation of the tail lobe near 1530 at a location within 2 R_E of the expected location of the tail neutral sheet.

Figure 3. Magnetic field data from two spacecraft separated by a large X distance. Both spacecraft remain in the tail lobe except for brief intervals near 16:30 and 20:00 when a dashed line for IMP-6 indicates the field equivalent contribution by the plasma. Data indicate how a tail energy decrease at both spacecraft is typically associated with a large AE increase.

Figure 4. Showing magnetic field data and its relations to θ_{IP} and a substorm. The vertical dashed lines at ~ 0425 and 0438 indicate the times of B_z increases associated with substorm onsets.

Figure 5a. Magnetic field data during a period with three substorms. The sudden increases in B_z at 0521 and 0901 is characteristic of distances inside ∿ 15 R_E while the slower change in B_z near 0000 is characteristic of larger distances.

Figure 5b. Plasma data for the same interval as 5a. Inside of 15 R_E, β at IMP-6 increases soon after onsets at 5:10 and 8:50 whereas at 19 R_E it is delayed by 80 minutes relative to the 0001 onset.

Figure 6. Magnetic field data at distant and near earth locations. Near earth increases in B_z correspond to substorm onsets but the plasma sheet recoveries are delayed relative to onset due to the IMP-6 location away from the equatorial plane.

Figure 7a. Magnetic field data during a period of substorms followed by a quiet interval. Three instances of plasma sheet thinning observed near the equatorial plane correspond to three substorms.

Figure 7b. Plasma data for the interval of 7a. The quiet interval is apparently caused by a northward θ_{IP} and it corresponds to an interval of cooling magnetotail plasmas.

Figure 8a. Magnetic field data illustrating plasma sheet thinning seen by two widely separated spacecraft near the equatorial plane. Just after 1100 during substorm recovery the plasma sheet reappears at times that correspond within 6 minutes at the two spacecraft. An unusually quiet interval occurs during an interval of northward field and corresponds to substantial northward B_z components in the tail.

Figure 8b. Plasma data for the interval shown in 8a. A gradual cooling of both electrons and ions can be seen during the quiet interval.

IMP 8	X=-18.4	-20.7	-22.8	-24.7	-26.4	-27.9	-29.2
	Y=16.8	15.1	12.8	10.0	7.4	5.3	3.7
	Z'=5.8	5.0	5.3	6.2	7.2	7.8	7.6
IMP 6	X=-22.0	-23.5	-24.8	-25.9	-26.9	-27.6	-28.2
	Y=12.6	12.4	12.6	13.1	13.4	13.3	12.7
	Z'=-1.5	-3.7	-4.3	-3.3	-1.8	-1.0	-1.8

NOVEMBER 1-2, 1973

Figure 1a

		X= -18.4	-20.7	-22.8	-24.7	-26.4	-27.9	-29.2
IMP 8		Y = 16.8	15.1	12.8	10.0	7.4	5.3	3.7
		Z' = 5.8	5.0	5.3	6.2	7.2	7.8	7.6
IMP 6		X = 22.0	-23.5	-24.8	-25.9	-26.9	-27.6	-28.2
		Y = 12.6	12.4	12.6	13.1	13.4	13.3	12.7
		Z' = -1.5	-3.7	-4.3	-3.3	-1.8	-1.0	-1.8
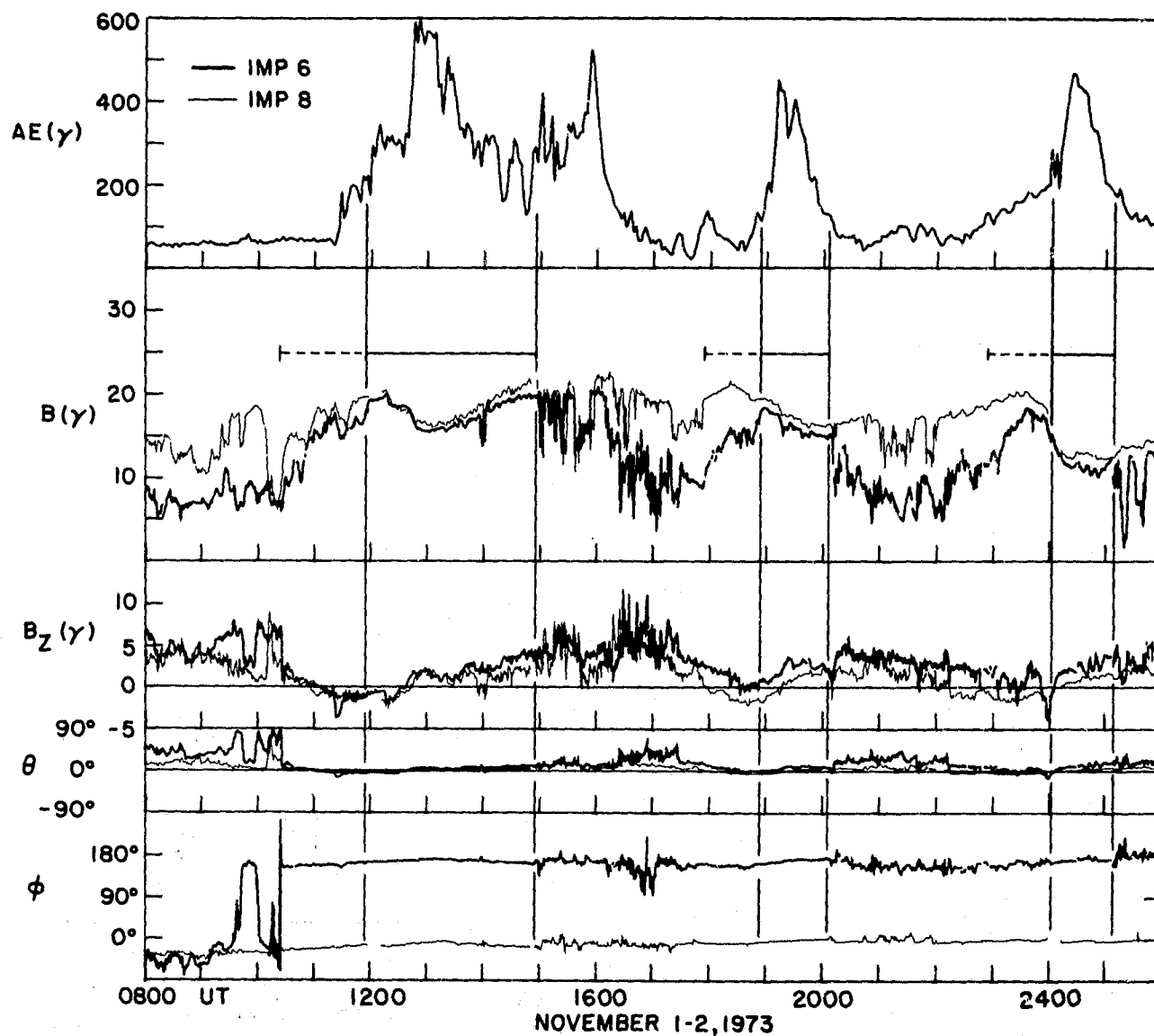
Figure 1b

IMP 8	X = -18.8	-21.1	-23.2	-25.1	-26.2
	Y = 18.2	15.9	13.7	12.5	11.9
	Z' = 5.4	7.5	9.0	9.0	8.1
IMP 6	X = -16.6	-18.3	-19.7	-21.0	-21.7
	Y = 16.5	17.4	18.0	-21.0	-21.7
	Z' = -2.0	-0.3	1.0	-0.4	-1.2

NOVEMBER 13-14, 1973

Figure 2a

	X =	-18.8	-21.1	-23.2	-25.1	-26.2
IMP 8	Y =	18.2	15.9	13.7	12.5	11.9
	Z' =	5.4	7.5	9.0	9.0	8.1
	X =	-16.6	-18.3	-19.7	-21.0	-21.7
IMP 6	Y =	16.5	17.4	18.0	18.5	18.6
	Z' =	-2.0	-0.3	1.0	-0.4	-1.2

IMP 8
IMP 6

$AE\,(\gamma)$

800
600
400
200

$B\,(\gamma)$

40
30
20
10

$B_Z\,(\gamma)$

10
0
-10

θ

90°
0°
-90°

ϕ

270°
90°
-90°

15:00   18:00   21:00   00:00   2:00

NOVEMBER 13-14, 1973

Figure 2b

IMP 8	X	-34.3	-34.6	-34.9
	Y	8.5	10.2	11.4
	Z'	-18.4	-18.1	-17.2
IMP 6	X	-9.2	-8.6	-7.8
	Y	15.6	14.5	18.3
	Z'	-9.9	-7.1	-4.2

AE(γ)

$P_{IP} \times 10^8$
(DYNES/cm^2)

θ_{IP}

B(γ)

B_z

θ

φ

DECEMBER 23, 1973
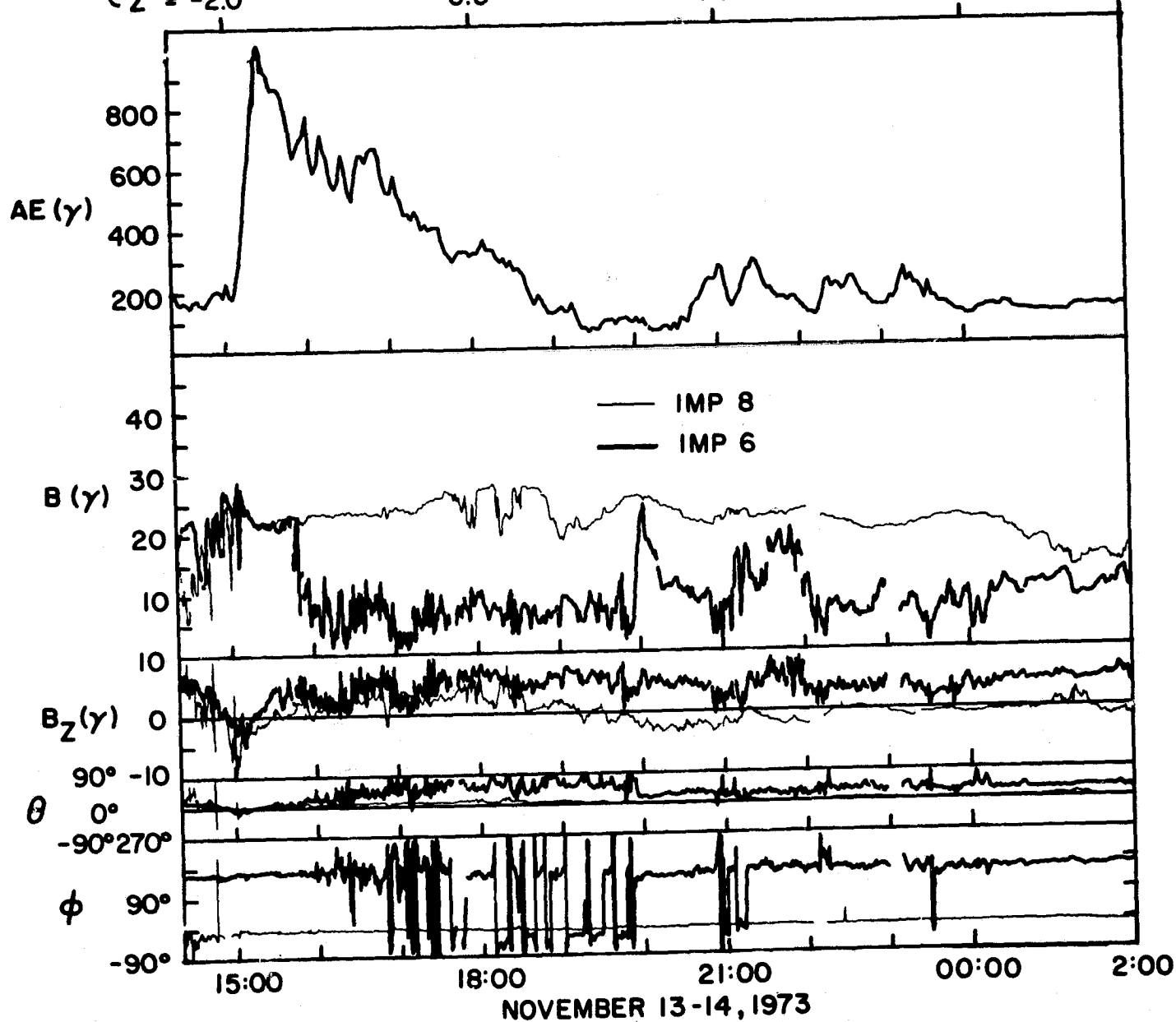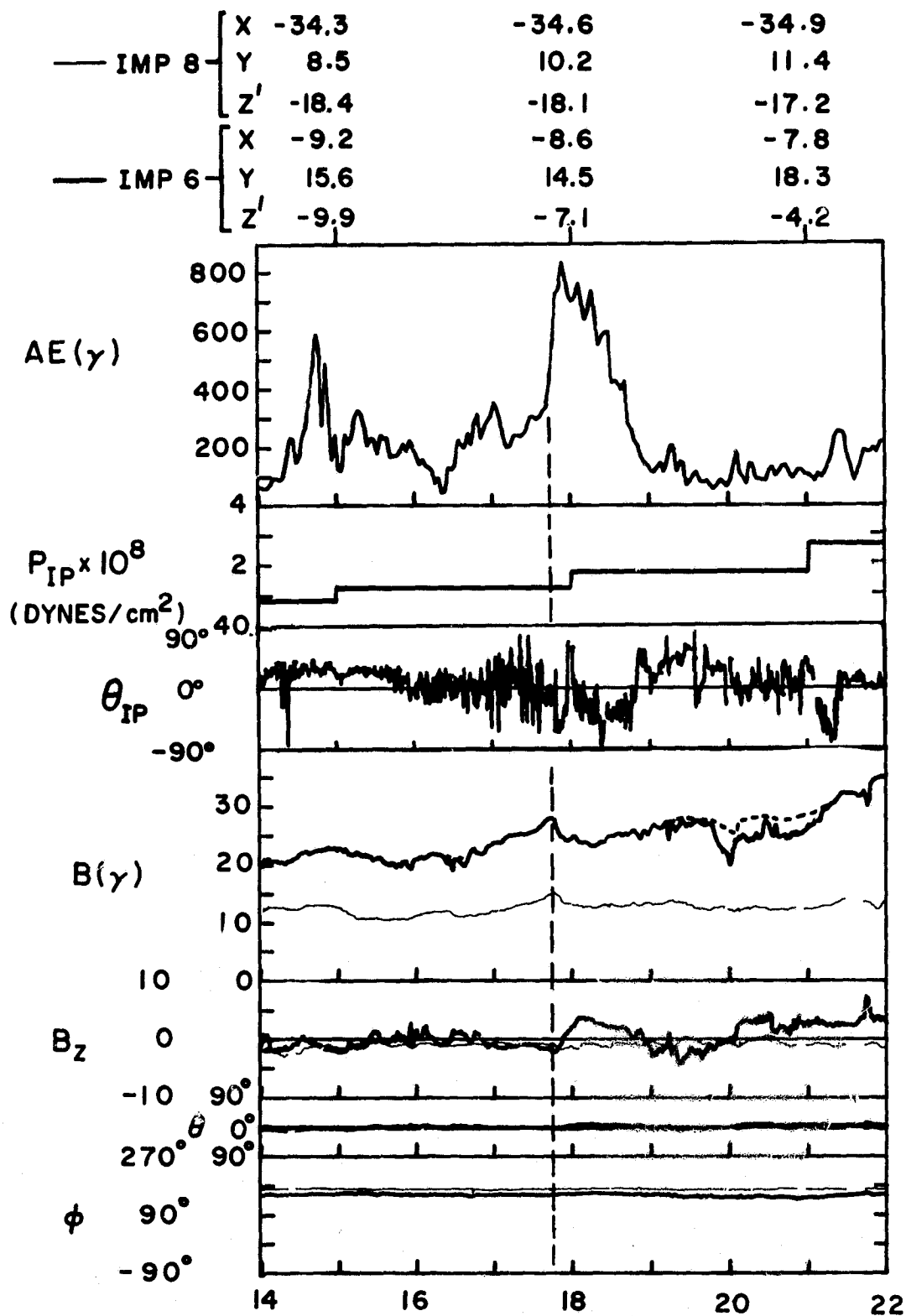
Figure 3

	X = -34.1	-34.2	-34.2
--- IMP 7	Y = 0.9	-0.9	-2.6
	Z' = 5.9	6.2	6.0
--- IMP 6	X = -10.4	-13.6	-16.4
	Y = 7.5	9.0	10.4
	Z' = 10.5	10.6	8.6

AE(γ) 400 200

θ$_{IP}$ 90° 0° -90°

B(γ) 30 20 10 0

B$_Z$(γ) 10 0 0 -10

θ 90° 0° -90°

φ 270° 90° -90°

0 3 6

OCTOBER 15, 1972

Figure 4

— IMP 7	X = -28.3	-29.5	-30.6	-31.5	-32.1
	Y = 16.8	15.9	14.8	13.1	11.8
	Z' = 10.2	8.5	6.0	4.1	3.2
— — IMP 6	X = -17.4	-14.3	-10.6	-6.2	-2.5
	Y = -3.5	-4.7	-6.0	-6.3	-5.4
	Z' = -4.5	-3.2	-2.4	-2.3	-2.3
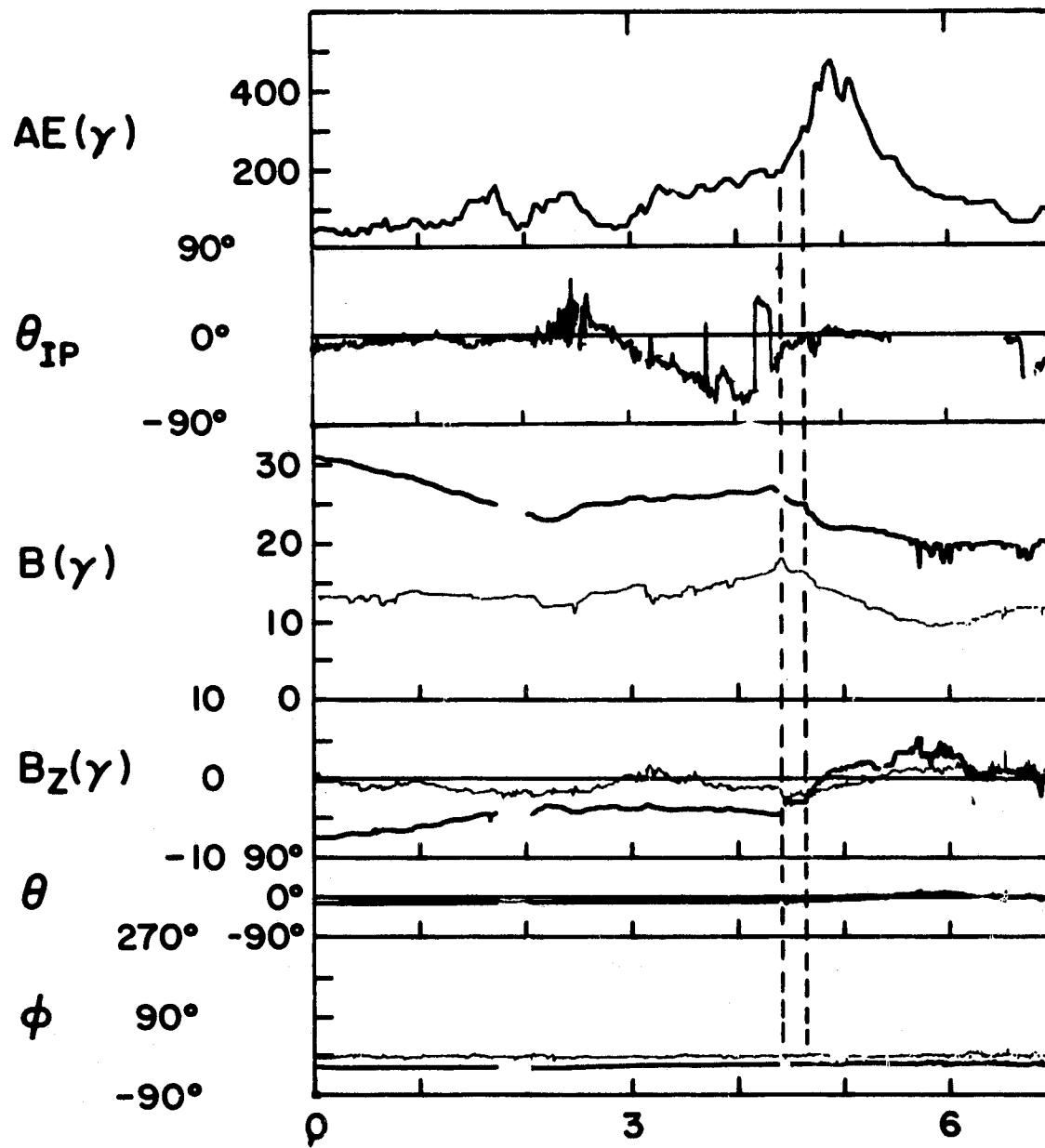
OCTOBER 14, 1972
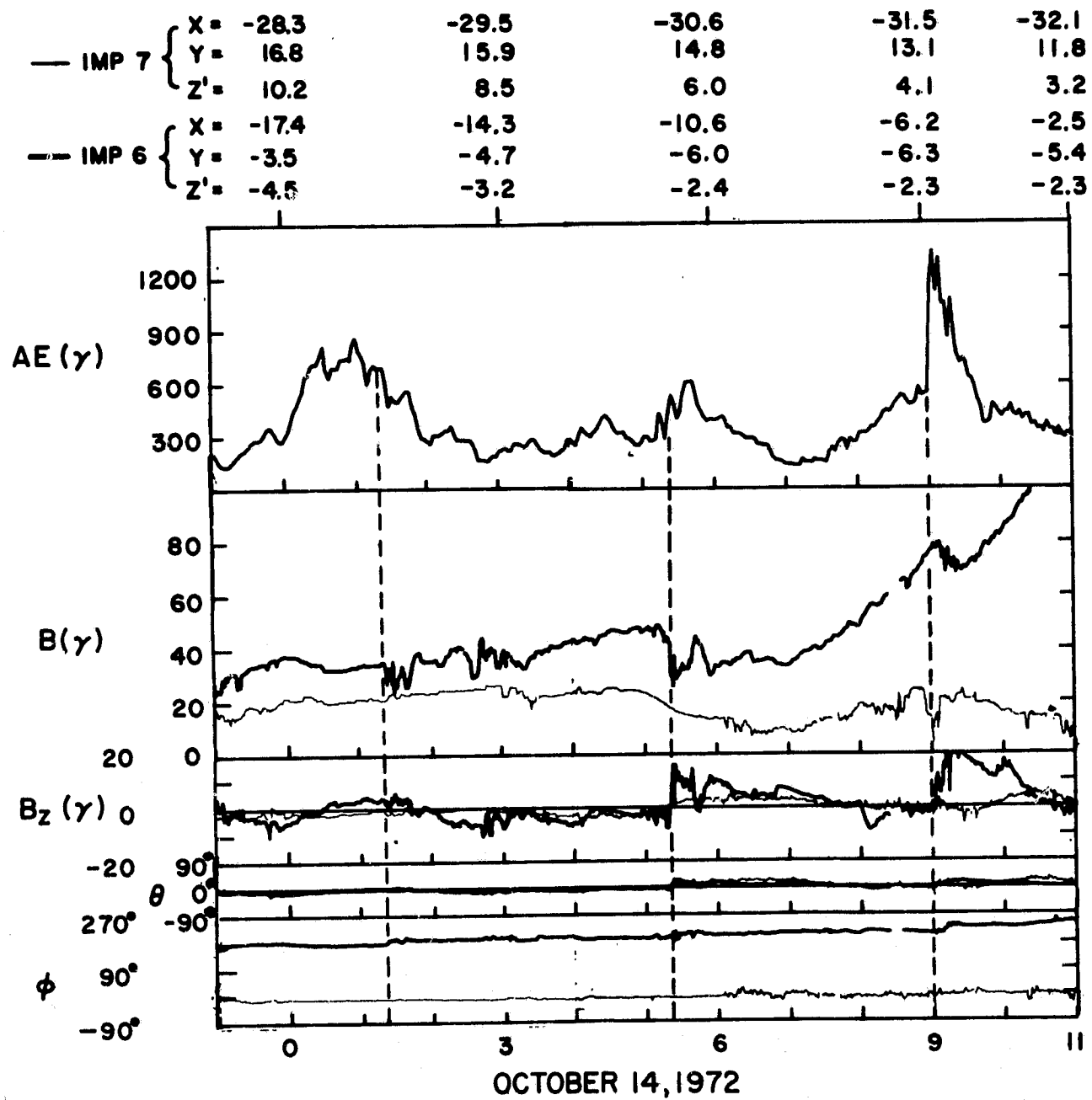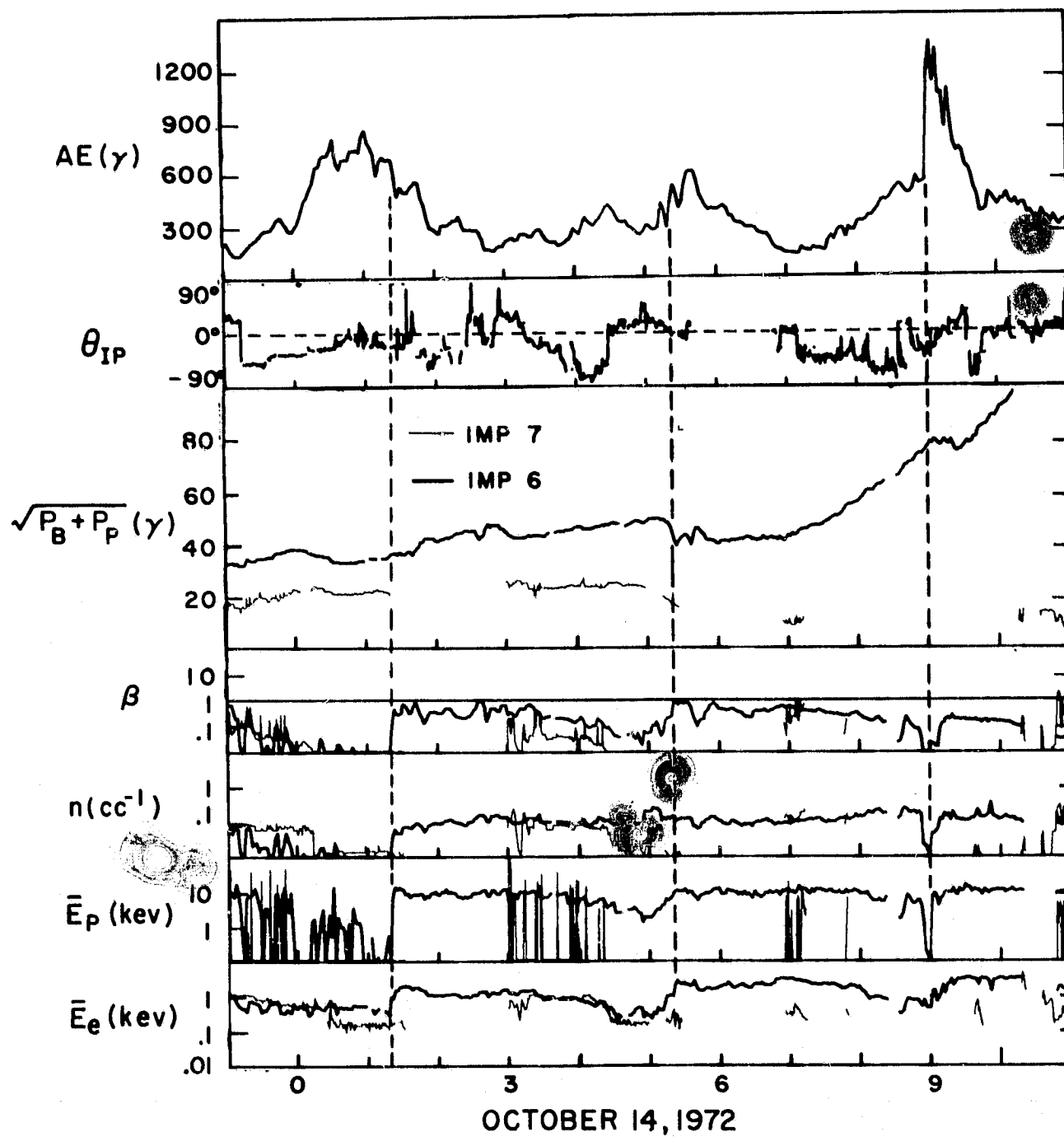
Figure 5a

Figure 5b

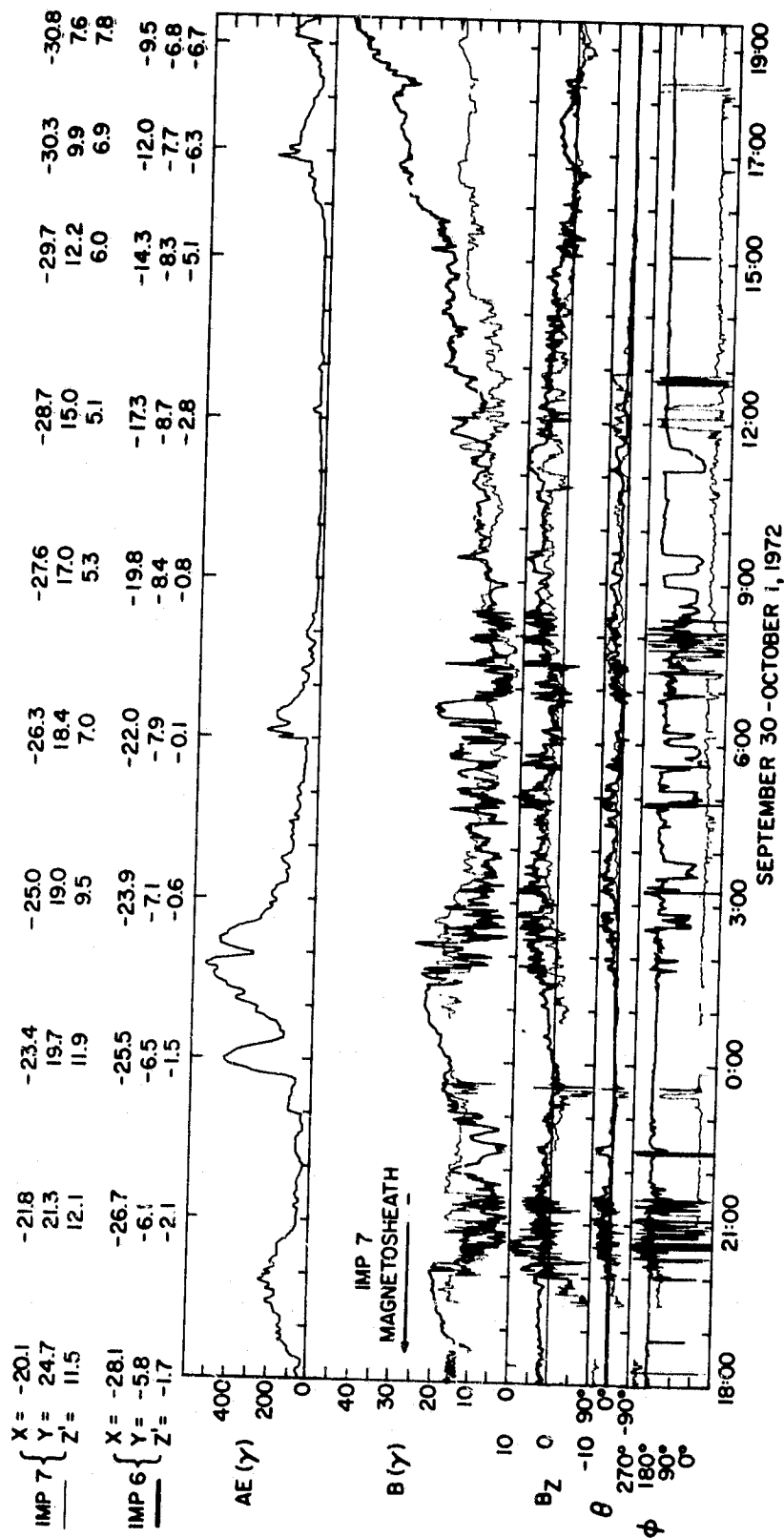| —IMP 8 | X = | -36.3 | -35.9 | -35.4 | -34.8 |
	Y =	-8.3	-7.9	-10.0	-14.6
	Z' =	-17.9	-18.6	-18.7	-19.4
—IMP 6	X =	-14.6	-12.7	-10.5	-7.7
	Y =	9.7	8.3	5.4	1.4
	Z' =	-8.2	-5.7	-3.9	-2.2
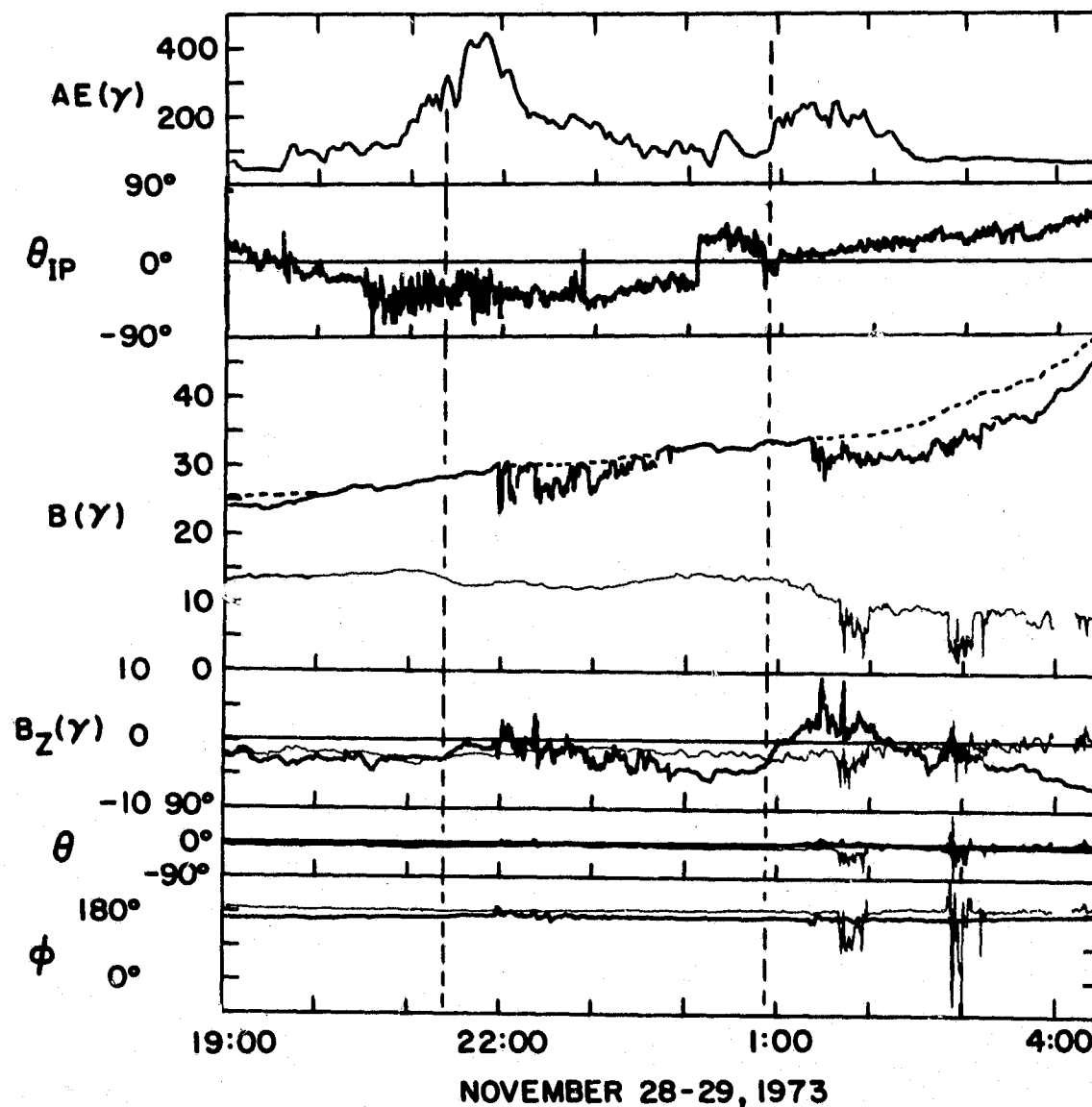
Figure 6

Figure 7a

Figure 7b

Figure 8a

Figure 8b